For ONR reporting purposes only. Contains Georgia Tech Confidential Information.

MURI: TEMPLATION OF LONG-CHAIN SEQUENCE-CONTROLLED HETEROPOLYMERS

SETH R. MARDER, BERNARD KIPPELEN, JOSEPH W. PERRY, MARCUS WECK
School of Chemistry & Biochemistry
School of Electrical and Computer Engineering
Center for Organic Photonics and Electronics
Georgia Institute of Technology
901 Atlanta Drive
Atlanta, GA 30332-0400

Phone: 404-385-6048
Fax: 404-385-6057
E-mail: seth.marder@chemistry.gatech.edu

September 30, 2008

Precise Materials by Nanopatterning

1: Selective growth of TiO_2 on nano patterned region

2: Application of thermochemical nanolithography to graphene oxide based devices

Index

Chapter I. Selective growth of TiO_2 on nano patterned region

1. Introduction

Titanium dioxide (TiO_2) has good properties, such as high refractive index (2.6 for rutile structure and 2.3 for anatase structure),[1] high dielectric permittivity (88 ~ 120),[2] appropriate band gap to absorb the ultraviolet, and stability to chemical erosion. Therefore, TiO_2 thin films are of interest for various applications including microelectronics, optical cells, solar energy conversion, highly efficient catalysts, microorganism photolysis, antifogging and self-cleaning coatings, gratings, gate oxides in metal-oxide-semiconductor field effect transistor, etc. Among these applications, TiO_2 for photocatalyst is spotlighted due to green chemistry in nowadays. It is reported that photo-oxidation reaction activity is in the order of TiO_2 (anatase), TiO_2 (rutile), ZnO, ZrO_2, SnO_2, and V_2O_3. So, TiO_2 with anatase structure is adequate to highly efficient photocatalyst. In order to increase the efficiency of photocatalyst, it is needed to increase TiO_2 surface area. Therefore, it is thought that nano structure of TiO_2 is well matched. But, it is difficult to align the nano materials to the purposed region. So, we wanted to grow nano structured TiO_2 selectively in the purposed region. To do this, the patterning technique with high speed and high resolution is needed. So, we chose thermo chemical nano lithography (TCNL) method. Therefore, we try to grow TiO_2 selectively in nano patterned region which is made by TCNL. Figure I-1 shows well the schematic experiment procedure in this experiment.

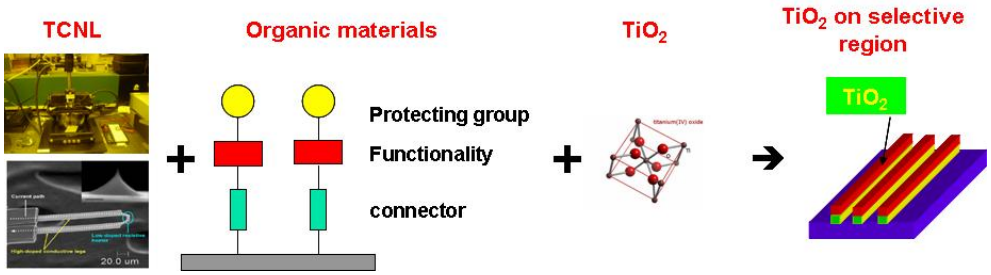

Fig. I-1 Schematic procedure of this experiment

Various attempts have been made to fabricate thin films and micropatterns of TiO_2 by several methods, and in particular, to synthesize materials and devices including TiO_2 thin films from an aqueous solution through an environment-friendly synthesis process, i.e., ‘‘green chemistry’’. It is reported that TiO_2 can be deposited by the use of titanium dichloride diethoxide and toluene.[3] Also, TiO_2 can be deposited by the use of solution containing ions such as TiF_6^{2-} and BO_3^{2-}.[4] For a start, we try to deposit TiO_2 using the solution containing ions such as TiF_6^{2-} and BO_3^{2-}.

2. Selective growth of TiO_2 on nano patterned region

2.1. Plan

2-tetrahydropyranyl N-(3-propyl triethoxy silane) carbamate and/or poly(2-tetrahydropyranyl N-(2-ethylmethacrylate) carbamate)-poly(methyl 4-(3-methacryloyloxpropoxy) cinnamate) will be used as a coating material on Si substrate. After TCNL treatment on this sample, the treated region will be changed from -THP group to $-NH_2$ bond. Then, $-NH_2$ bond can be changed to $-CH_3$ bond using octyl

isocyanate. After that, TiO_2 cannot be deposited on -CH_3 bond, i.e. octyl isocyanate, but it can be deposited on -THP bond, i.e. 2-tetrahydropyranyl N-(3-propyl triethoxy silane) carbamate. This schematic procedure is well depicted in Fig I-2.

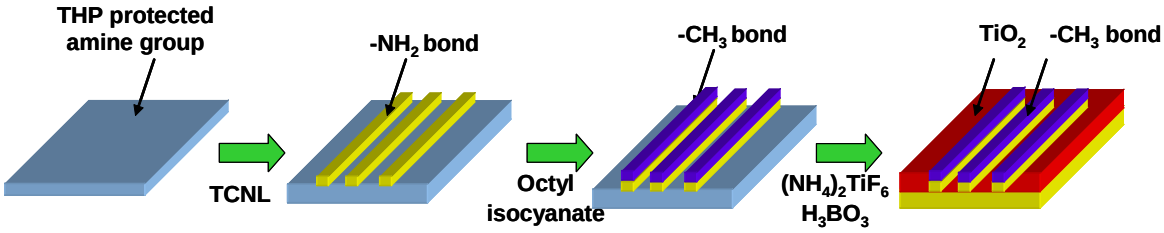

Fig. I-2 Plan I: The method to grow TiO_2 on nano patterned region

The advantage of this plan is that it is simple process. But, it is afraid that if the size of TiO_2 is big, it would cover the nano patterned region so that pattern could not be recognized well. So, another plan is also considered, as shown in Fig. I-3. The -THP protected amine organic materials also will be used as coating materials. After TCNL treatment on this sample, patterned region will change to -NH_2 bond. Then, -NH_2 bond can be changed to -CHO bond using glutaraldehyde. After that, -THP ending group can be changed to -NH_2 through the heating process. Then, we will change -NH_2 bond to -CH_3 bond using octyl isocyanate. If this sample is dipped into $(NH_4)_2TiF_6$ and H_3BO_3 solution, it is expected that TiO_2 can be grown on only -CHO group, not on -CH_3 group. The advantage of this experiment is that it is easy to find the pattern. But, this process is little bit complicate in comparison with former process.

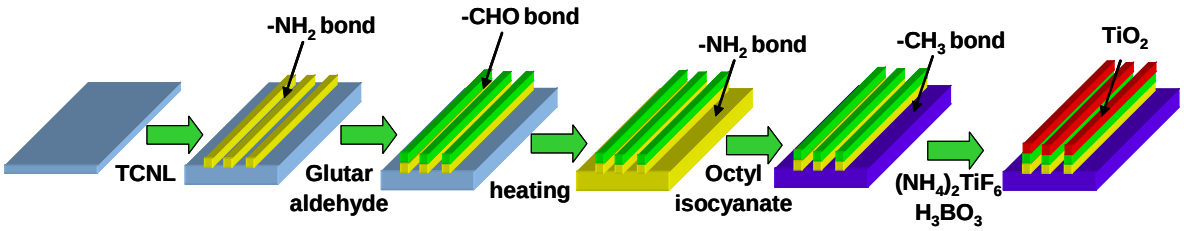

Fig. I-3 Plan II: The method to grow TiO_2 on nano patterned region

2.2. TCNL treatment on Will's polymer

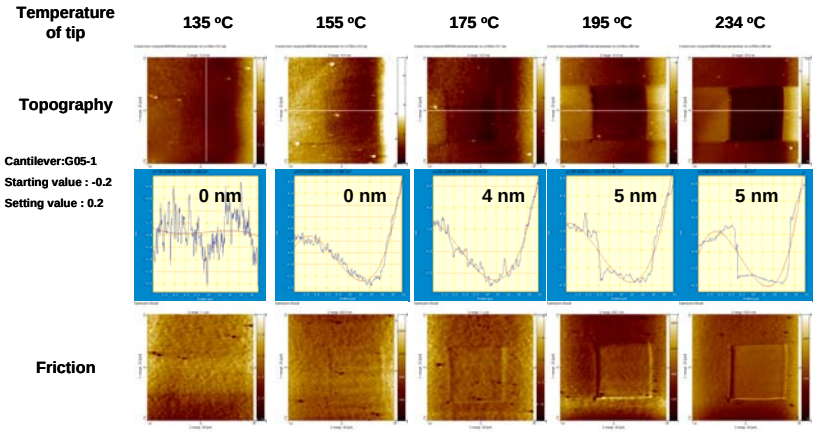

Fig. I-4 The change of topography and friction images as a function of TCNL tip temperature on Will's polymer (WDU-II-1456)

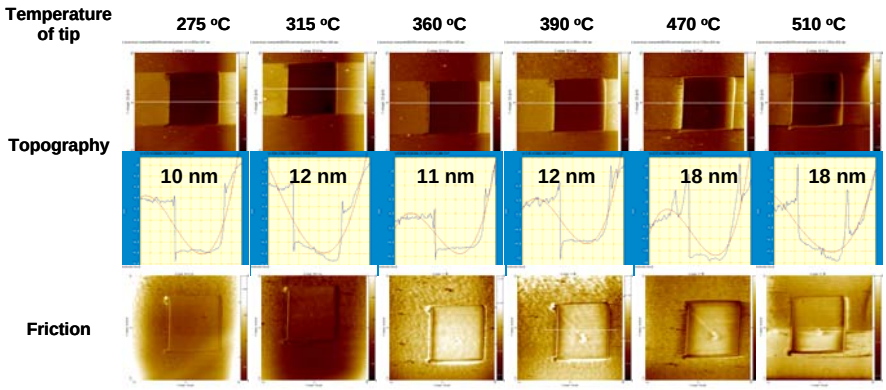

Fig. I-5 The change of topography and friction images as a function of TCNL tip temperature on Will's polymer (WDU-II-1456)

Figure I-4 and I-5 shows the result of TCNL treatment on Will's polymer (WDU-II-1456). The heated area is 10 × 10 μm^2. G05-1 cantilever was used in this experiment. Starting deflection value and setting deflection value are - 0.2 and 0.2, respectively. The indentation is found after the temperature of tip increased over than 175 ^oC. It seemed that the depth of indentation increased with the temperature. Furthermore, the increase of fiction force is clearly seen after the temperature of tip increased over than 360 ^oC. From this experiment, it is found that pattern on polymer can be made well using TCNL.

2.3. TCNL treatment on Jonas' SAM

Figure I-6 shows the result of TCNL treatment on Jonas' SAM. The heated area is also 10 um x 10 um, as shown in red box. The indentation is not found because SAM is too thin. Honestly, the change of friction force is expected, but it is in vain even if 400 ^oC is applied. It is thought that further experiments are needed to deprotect THP from the SAM and to detect the change of friction force after TCNL treatment.

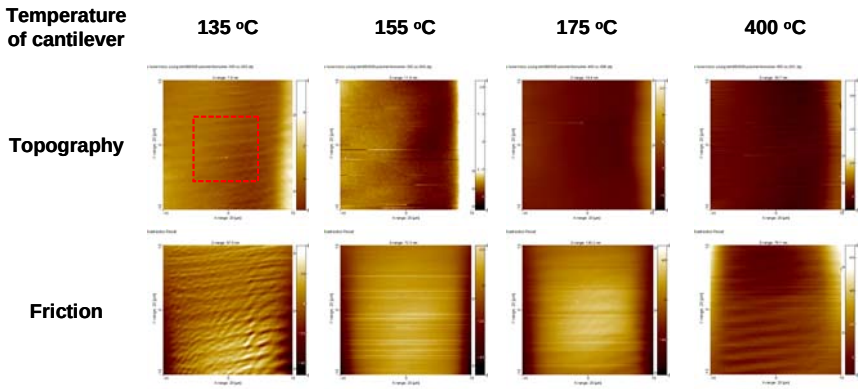

Fig. I-6 The change of topography and friction images as a function of TCNL tip temperature on Jonas' SAM

2.4. Deposition of TiO_2 on Jonas' SAM patterned by TCNL

Using patterned Jonas' SAM, we deposited TiO_2. The patterned area is 10×10 μm^2. We made only one pattern and made mark near the patterned area to recognize. To be honest, it is thought that only one pattern is good for our experiment because it is easy to recognize. However, it turned out that it not easy to recognize because deposition is not uniform.

Scheme 1 procedure is to deposit TiO_2 on Si surface except for patterned area. As shown in Fig. I-7, TiO_2 did not deposit on patterned area, but the deposition is not uniform. So, further experiments are needed to improve selectivity. Scheme 2 procedure is to deposit TiO_2 only on patterned region. TiO_2 deposited on patterned area, but the deposition is not uniform either, as shown in Fi.g I-7. So, further experiments are needed.

Through this experiment, it turned out that deposition of TiO_2 is not reproducible and it is not easy to find the patterned region. The method to solve problems is to make many patterns to recognize easily and to make SAM or polymer on Si patterned with grid to find the location easily. We are doing this experiment now.

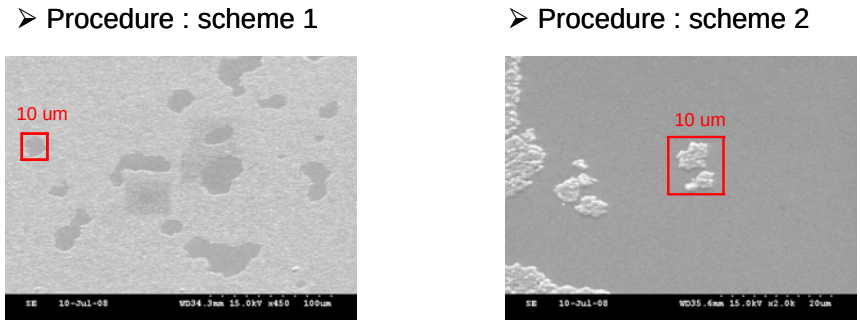

Fig. I-7 Selective deposition of TiO_2 on nano patterned region

3. X-ray diffraction (XRD) measurement

3.1. TiO_2 grown on Will's polymer

Figure I-8 shows the XRD spectra of TiO_2 on different kinds of samples. In this experiment, TiO_2 grown on Will's polymer, glutaraldehyde, and octyl isocyanate (OIC) were used. Will's polymer without deposition of TiO_2 was also used as a reference. TiO_2

(004) peak was found on the surface of Will's polymer and glutaraldehyde, but OIC. This result also supports that TiO_2 can be grown Will's polymer and glutaraldehyde, but OIC. It is thought that the peak intensity is so low because TiO_2 is not crystallized well.

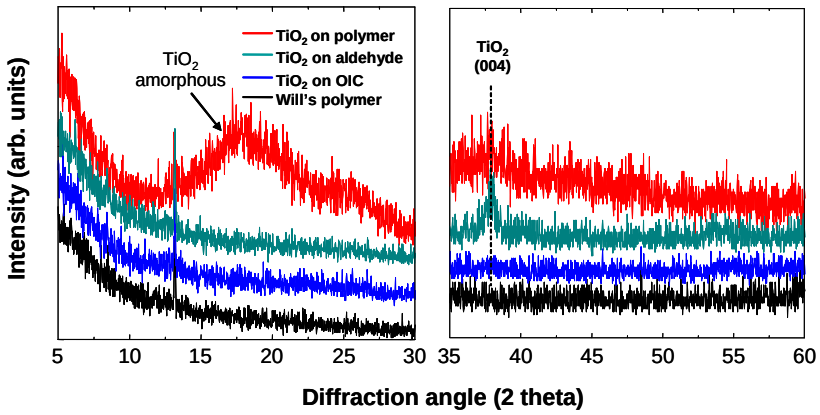

Fig. I-8 XRD spectra of TiO_2 on Will's polymer spincoated on Si

3.2. TiO_2 grown on Jonas' SAM

Figure I-9 shows the XRD spectra of TiO_2 on different kinds of samples. In this experiment, we used Jonas' SAM, Jonas' SAM heated at 210 ^oC for 20 min, APTES, and Bare Si after deposition of TiO_2. It seems that TiO_2 was grown in all samples. XRD patterns showed the same tendency regardless of the type of SAM. TiO_2 (101), TiO_2 (004), and TiO_2 (200) peaks were shown at 25.3^o, 37.8^o, and 48.0^o, respectively, indicating that TiO_2 has anatase structure. It is thought that the peak intensity is so low because TiO_2 is not crystallized well.

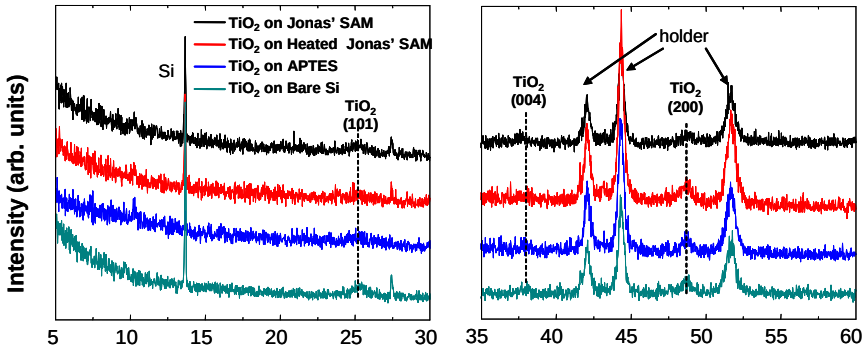

Fig. I-9 XRD spectra of TiO_2 on Jonas' SAM immobilized Si

Figure I-10 shows the XRD spectra of TiO_2 on different kinds of samples. In this experiment, TiO_2 grown on glutaraldehyde and OIC which are immobilized in Jonas' SAM were used. Jonas' SAM without deposition of TiO_2 was also used as a reference. It seems that TiO_2 was grown on glutardaldeyde, but it is not clear. This result also supports that TiO_2 can be grown glutaraldehyde, but OIC. It is thought that the peak intensity is so low because TiO_2 is not crystallized well.

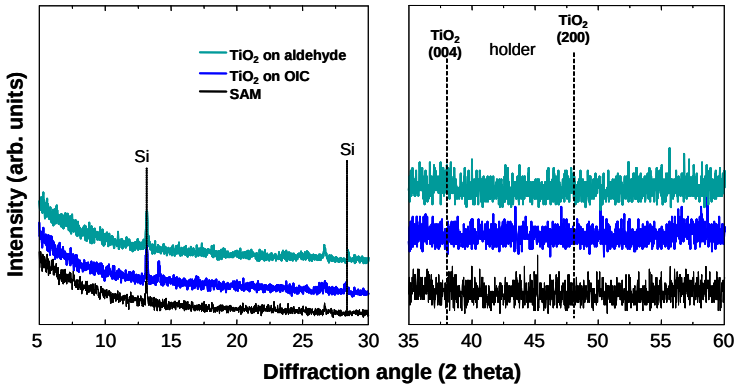

Fig. I-10 XRD spectra of TiO_2 on Jonas' SAM immobilized Si

4. Selective growth of anatase TiO_2 on amorphous TiO_2

4.1. Literature survey

According to the reference paper (Fig. I-11), it is reported that TiO_2 can be grown selectively on amorphous TiO_2 under pH 1.5. They used Si wafer. OTS-SAM was coated on Si wafer. After that, UV was irradiated on OTS-SAM to change CH_3 group to OH bond using mask. 0.1 M titanium dichloride dietoxide and anhydrous toluene were used to deposit amorphous TiO_2 as a seed layer under N_2 ambient in glove box. Finally, $(NH_4)_2TiF_6$ and H_3BO_3 were used to deposit anatase TiO_2. They found that anatase TiO_2 was grown selectively on amorphous TiO_2. So, we tried this method to increase the selectivity and this experiment is still on going.

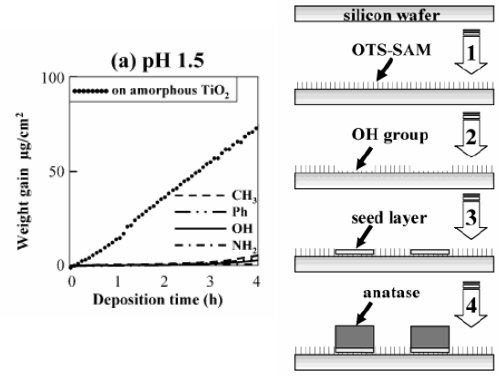

Y. Masud *et al.* Langmuir 19 (2003) 4415

Fig. I-11 The method to increase selectivity

4.2. SEM data of amorphous TiO_2

Figure I-12 shows the SEM images of amorphous TiO_2. From the SEM images and EDS spectra, it is shown that amorphous TiO_2 can be grown well on SiO_2, APTES, THP protected amine SAM, and THP protected amine SAM heated at 210 ^oC. However, TiO_2 is not grown on OTS, indicating that TiO_2 cannot be grown on CH_3 bonding group. This result is same to ours. The deposition of anatase TiO_2 on amorphous TiO_2 is still on going now.

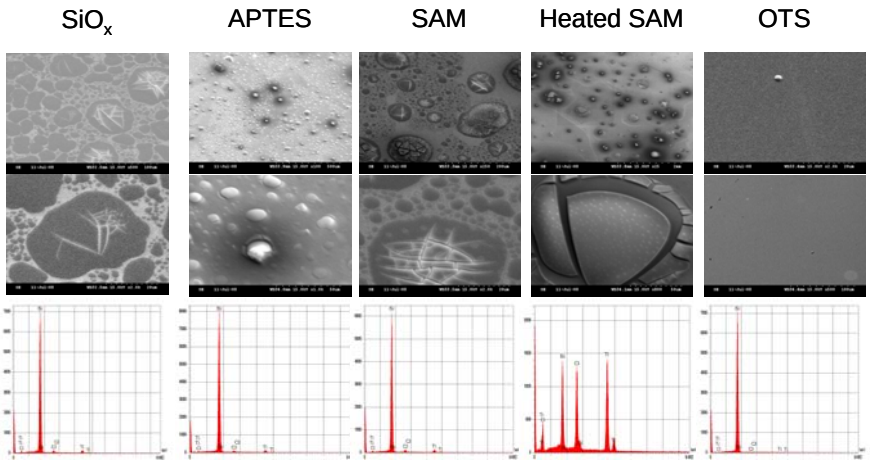

Fig. I-12 SEM images of amorphous TiO_2

5. Conclusion

The selective growth of TiO_2 was tried. Nano patterns were made on Will's polymer by TCNL technique. However, further experiments are needed to make pattern on Jonas' SAM by TCNL. According to XRD spectra, the structure of all TiO_2 grown by LPD method is anatase regardless of surface functionality. Furthermore, XRD data convinced that TiO_2 can be grown on -THP, -OH, and -CHO, but $-CH_3$ bond. In order to increase possibility of selective growth of TiO_2, we would like to combine LPD method with sol-gel method. From these results, we expect that TiO_2 can be grown selectively on nano patterned region.

6. Future plan

It is known that TiO_2 can be grown selectively. So, we want to deposit TiO_2 on the nano patterned region by TCNL. If the surface is not uniform after deposition of TiO_2, it will not be easy to recognize the exact location where patterns were made. Therefore, the way to recognize patterned region easily will be investigated. Eventually, the growth of TiO_2 on the patterned region will be tried. Additionally, we will characterize the properties of TiO_2 using XRD, XPS, and EDS. After that, we will apply other oxides (ZnO_2, SnO_2, or V_2O_5) to the selective growth

Ultimately, our final purpose is the selective growth of n-type nano rod, such as ZnO, CdSe, and SiGe, on the patterned region of p-type semiconductor substrate by TCNL in order to utilize the nano quantum device using p-n junction.

7. References

[1] I. Oja, A. Mere, M. Krunks, R. Nisumaa, C.-H. Solterbeck, and M. Es-Souni, Thin Solid Film **515**, 674 (2006).
[2] S. A. Campbell, D. C. Gilmer, X.-C. Wang, M.-T. Hsieh, H.-S. Kim, W. L. Gladfelter, and J. Yan, IEEE T. Electron Dev. **44**, 104 (1997).
[3] Y. Masuda, Y. Jinbo, T. Yonezawa, and K. Koumoto, Chem. Mater. **14**, 1236 (2002).
[4] Y. Masuda, W.-S. Seo, and K. Koumoto, Solid State Ionics **172**, 283 (2004).

Chapter II : Application of thermochemical nanolithography to graphene oxide based devices

1. Introduction

Recently, graphene has come to receive significant attention as a potential high mobility material for ultra-fast electronic device fabrication. Graphene means the one layer of carbon sheet which can be obtained after unrolling the carbon tube or scraping the graphite, as shown in Fig. II-1. In the case of carbon nano tube, it has some problems with placement and uniformity due to its shape. In the case of graphite, it is not easy to control the thickness of graphite. So, graphene has recently attracted attention. Furthermore, planar form of graphene has most of the desirable properties of nano tube and graphite.[1]

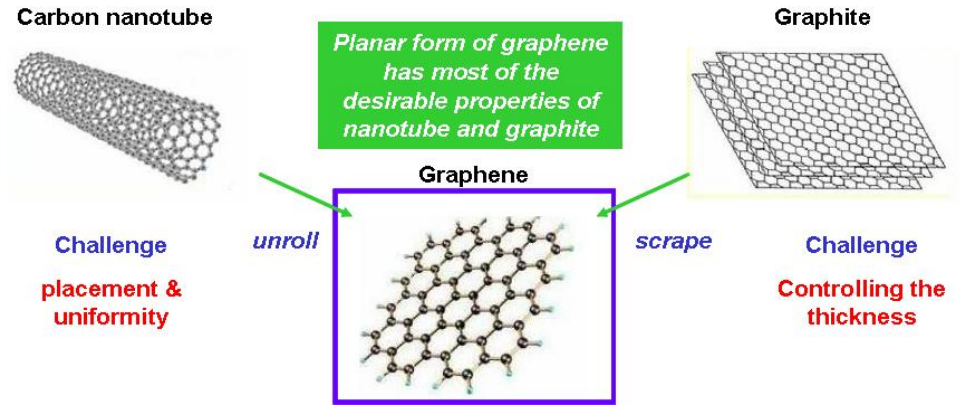

Fig. II-1 The definition of graphene

Graphene has sp_2 hexagonal structure and honeycomb lattices. Its atomic distance in horizontal plane is 0.25 nm and in vertical plane is 0.67 nm. It also has high mobility for both electrons and holes, which is ten times faster than that of Si. The mobility of graphene is over than 15,000 cm^2/Vs and its effective mass is $0.06m_0$. So, high current density could be obtained. Graphene has sub nm thickness which is lower than debye screening length so that it can be used in ideal electronics such as monolayer on insulator. Because planar processing can be used in the fabrication of graphene devices, we can expect the straightforward integration with CMOS. Therefore, we would like to use graphene or graphene oxide (GO) as device materials.

Fig II-2 shows the current-voltage curve after heating on GO which comes from prof. Walter de Heer group in physics department. When 10 volt was applied to the GO in as-deposited state, the current density is very low, indicating that GO in as-deposited state has insulting property. However, after heating at 180 ^oC for 16 hrs on GO, the current density increased compared with the current density in as-deposited state, indicating that the GO has semiconductor property. Therefore, this result suggested that the band gap of GO could be modulated by heat treatment. According to the previous result, GO loses oxygen when heated above 100 ^oC.[2] This means that the degree of oxidation can be adjusted by curing. So, it is thought that GO has semiconductor properties after heating at 180 ^oC for 16 hrs because GO lost the oxygen. Using this result, we intend to use GO as a field effect transistor materials.

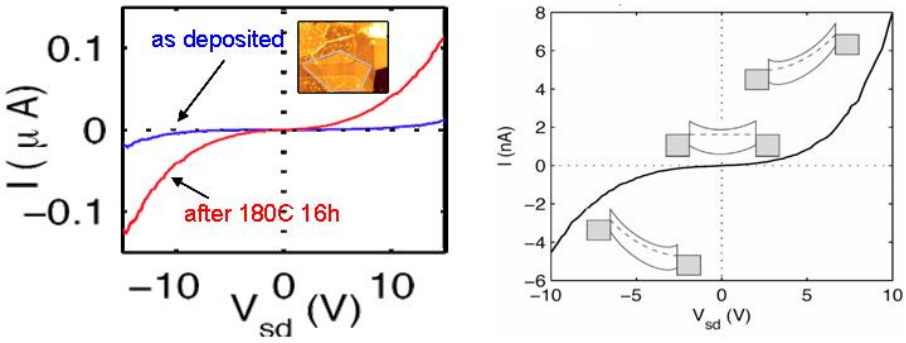

Fig. II-2 Current-voltage curve of GO after thermal treatment

However, significant challenges in the development and integration of graphene structures into functional electronic devices are remained. Fabrication of such small nanowires of graphene with sufficient control to produce uniform electrical property devices is extremely difficult using current microelectronics fabrication technologies. So, we would like to develop methods using tip-based nanofabrication that can produce such graphene nanowires in a facile and high throughput manner such that graphene transistor devices can be both effectively researched and ultimately practically implemented. Prof. Seth Marder group and prof. Elisa Riedo group have recently reported a new chemical nanolithography technique, i.e., thermo-chemical nanolithography (TCNL).[3] TCNL employs a resistively heated atomic force microscopy (AFM) cantilever to induce well-defined chemical reactions in order to locally change the surface functionality of thin films and self-assembled monolayers and to cause local chemical reactions to occur. This TCNL technique has been employed to write a controlled chemical pattern on a polymer surface with sub-15 nm resolution and at speeds up to 1.4 mm/s. Using TCNL method, we can apply heat to narrow region in GO to modulate the bandgap of GO. So, we will produce this thermally induced deoxidation process at the nanoscale locally by heating a GO film with a heated tip to directly create graphene nanowires of any desired dimension. Therefore, it is expected that we can make a nanodevices, such as nano FET, as shown in Fig. II-3.

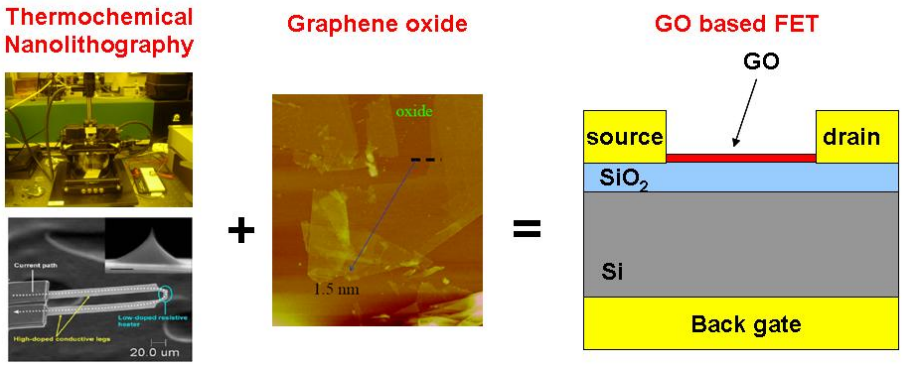

Fig. II-3 The purpose of this experiment

2. Factors which affect the formation of holes in GO

2.1. Basic principle of cantilever force

AFM cantilevers are consumption goods. Therefore, it is needed to check if same conditions can be applied to make holes on GO though tip is changed. In order to check this point, tip was changed from G04#3 to G05#1. In this case, same condition which was applied to make holes on GO using G04#3 was applied to GO using G05#1, but it did not work, as shown in Fig. II-4. Even if the applied voltage increased up to 15 V, which means the increase of temperature, pitch of GO was not found. So, the other concept to make a hole is introduced. Force is equal to spring constant multiplied by height difference, delta. It is thought that if the cantilever is changed, the spring constant of cantilever is also changed. Thus, different condition to make a hole should be applied to GO.

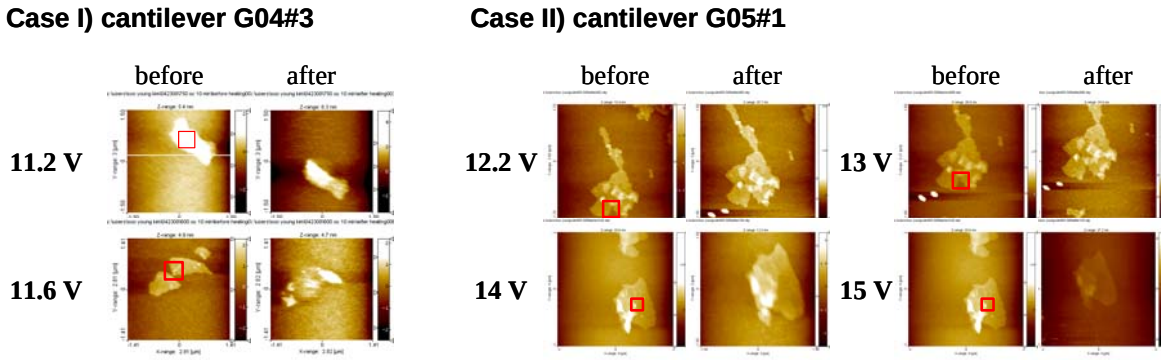

Fig. II-4 The effect of cantilever change on etching of GO

In order to understand the GO etching mechanism, it is needed to know the principle of cantilever force.

$$F = k \times \Delta = k(nm/nm) \times S_z(nm/V) \times V(V)$$

Cantilever force(F) is equal to spring constant of cantilever(k) multiplied by delta. Delta is defined by the multiplication of conversion factor(S_Z) and voltage(V). Spring constant and conversion factor are the fixed value which depends on the cantilever and piezoscanner. The only thing we can alter is the voltage. Voltage can be determined by the difference between starting deflection point(a) and setting deflection point(b), as shown in Fig. II-5. Starting deflection point can be fixed by adjusting laser diode. Its value has generally minus sign. As the cantilever approaches the sample and the force increases, the cantilever is supposed to be bent. Then, the reflected laser beam will move upside. The setting deflection value is the limit which stops cantilever approach to the sample. The setting deflection value is generally positive sign. Therefore, cantilever force can be controlled by adjusting the starting deflection point and setting deflection point.

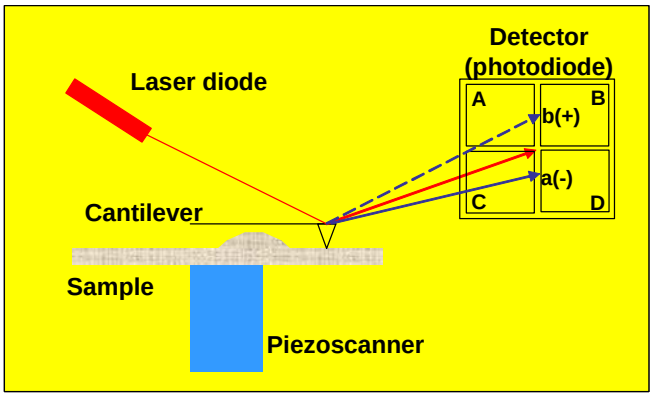

Fig. II-5 The principle of cantilever force

2.2. The effect of AFM setting deflection value on etching of GO

Figure II-7 shows the effect of AFM setting deflection value on etching of GO. In other words, the effect of cantilever force at same tip temperature is explored. The scan speed, starting deflection value, applying tip temperature, and number of scan time are fixed to be 997 nm/s, -0.2, 430 ^{o}C, and one time, respectively. Setting deflection value was changed from 0.2 to 2, meaning the increase of cantilever force. Red box indicated the region heated by TCNL tip. The pitch on GO was found if the setting deflection value is over than 1. This result indicates that applying force affect on the formation of pitch on GO.

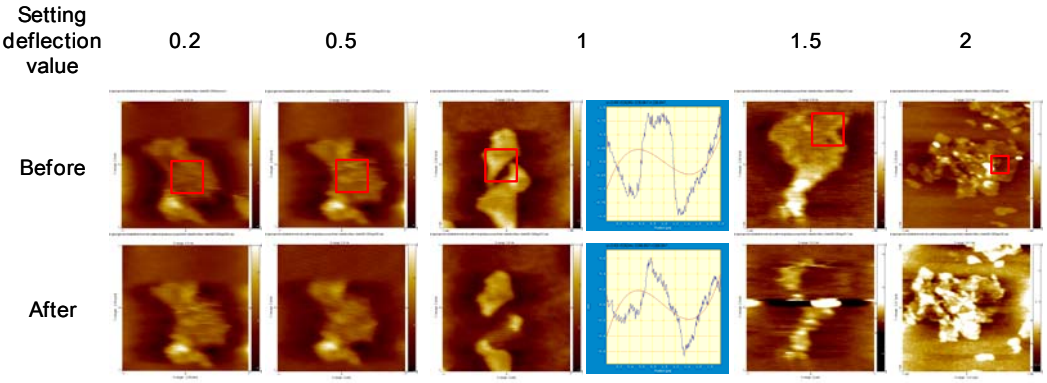

Fig. II-6 AFM topography images
after applying TCNL treatment with different setting deflection value (430 ^{o}C)

In order to make sure that applying force also affect on the formation of pitch in GO, the applying tip temperature increased from 430 ^{o}C to 500 ^{o}C. The scan speed, starting deflection value, applying tip temperature, and number of scan time are fixed to be 997 nm/s, -0.2, 500 ^{o}C, and one time, respectively. In order to change the cantilever force, setting deflection value was changed from 0.2 to 2. Red box which is shown in Fig. II-7 indicated the region heated by TCNL tip. The pitch on GO was not found until the setting deflection value increase over than 0.5. Therefore, it seems that force should be higher

than critical force to etch the GO, even if temperature is high enough. This result strongly suggested that applying force also affect on the formation of pitch on GO.

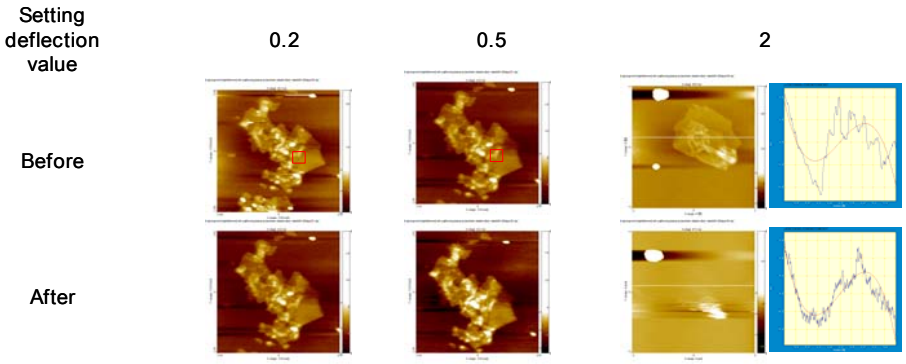

Fig. II-7 AFM topography images
after applying TCNL treatment with different setting deflection value (500 ^{o}C)

2.3. The effect of AFM starting deflection value on etching of GO

In order to check the effect of starting deflection value on etching of GO, our experiments were performed with changing the starting deflection value. The scan speed is 997 nm/s, setting deflection value is 1, applying tip temperature is fixed to 430 ^{o}C, and scan time is one. When starting deflection value is -0.2, pitch was made. However, pitch was not found after starting deflection value increased to 0. Since the difference between starting deflection value and setting deflection value is related to the cantilever force, this result support the hypothesis that the minimum force is needed to make a pitch even if the tip temperature is over than 430 ^{o}C.

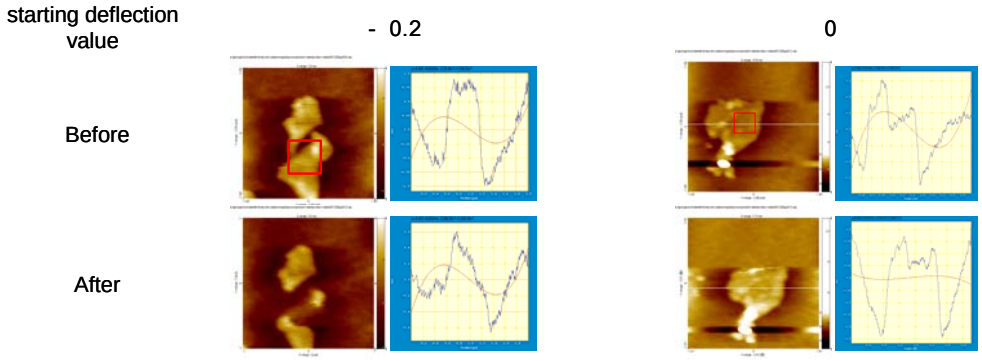

Fig. II-8 AFM topography images after applying TCNL treatment
with different starting deflection value (430 ^{o}C)

2.4. The effect of number of AFM scanning time on etching of GO

The effect of AFM scanning time on etching of GO is shown in Fig. II-9. The scan speed, starting deflection value, and applying tip temperature are fixed to 997 nm/s, -0.2,

and 430 ^{o}C. When the deflection value is set to 0.2 and only one scan is applied, the pitch could not be made. After applying the force on GO for 10 times, the pitch is found. In case the setting deflection value is 0.5, applying the cantilever force on GO for one time could not make a pitch, however, applying the force for five times could make a pitch on GO. This result indicated that formation of pitch on GO could be happened if number of scanning time increased although the force is not enough to etch the GO. Furthermore, it seems that the higher force is applied, the lower scanning time is needed. And, it seems that applying force is related with the depth of pitch in GO.

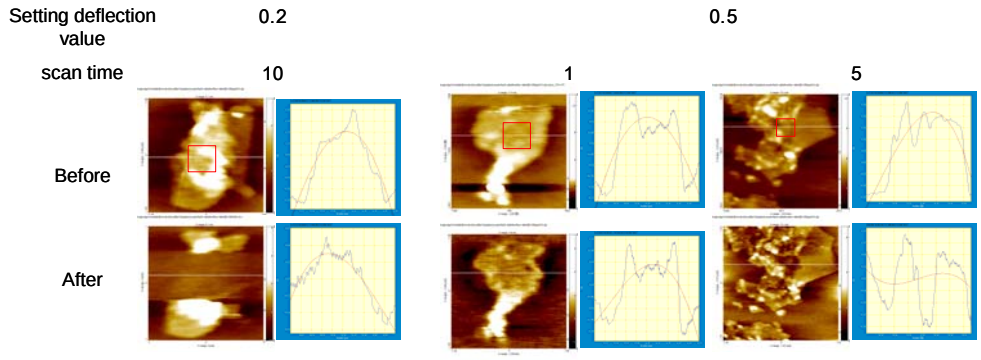

Fig. II-9 AFM topography images after applying TCNL treatment with different scanning times (430 ^{o}C)

3. GO versus HOPG

3.1. TCNL treatment on HOPG

In order to investigate the effect of TCNL on highly ordered pyrolytic graphite (HOPG), AFM images of HOPG were taken. Figure II-10 shows the topography and friction AFM images of HOPG without heating. The surface was changed while AFM measurements were conducted. This means that the applying the contact mode affects the location of debris on the surface so that it is need to be stabilized. Thus, HOPG was used after stabilization process.

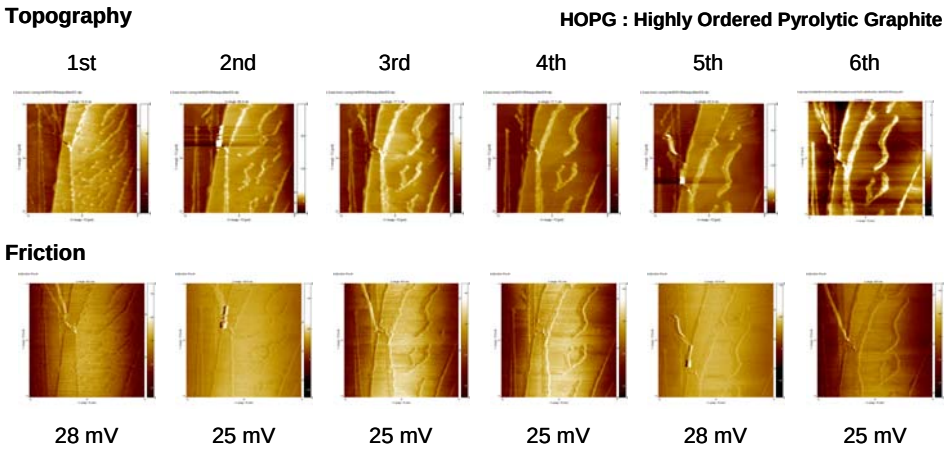

Fig. II-10 Stabilization steps for HOPG

Figure II-11 show the HOPG images after applying the TCNL whose tip temperature is 330 ^{o}C. The scanning speed was fixed to 1995 nm/s. This condition is same to the condition which can make holes on GO. Even after applying TCNL treatment on HOPG several times, the hole is not found. This result indicated that properties of HOPG are different from those of GO so that same condition to make holes cannot be applied.

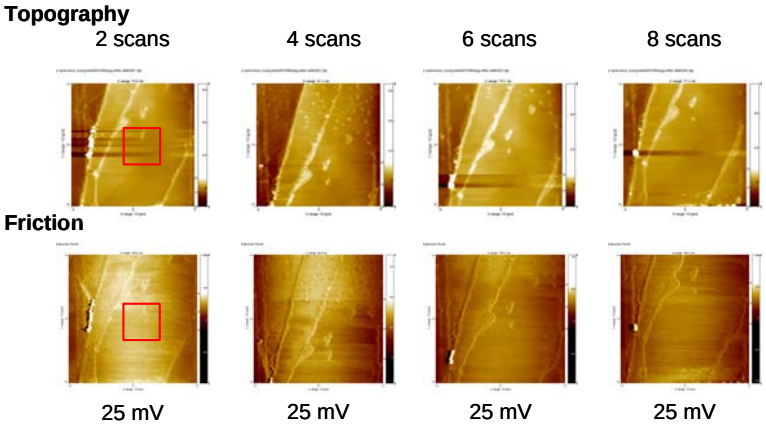

Fig. II-11 TCNL treatment on HOPG (330 ^{o}C)

Figure II-12 shows the direct comparison between GO and HOPG after TCNL treatment. This experiment was performed at 330 ^{o}C. G#04-6 tip was used. The starting deflection value and setting deflection value were set to -0.2 and 0.2, respectively. Sum value was 0.5. And, this experiment was performed after the surface of HOPG was stabilized. Red box indicates the exact location where TCNL tip contacted. Two holes were found in GO after TCNL techniques were applied to GO. However, the hole was not found on HOPG even though same TCNL experiment was applied to HOPG. This result indicated that there are many differences to make holes between GO and HOPG.

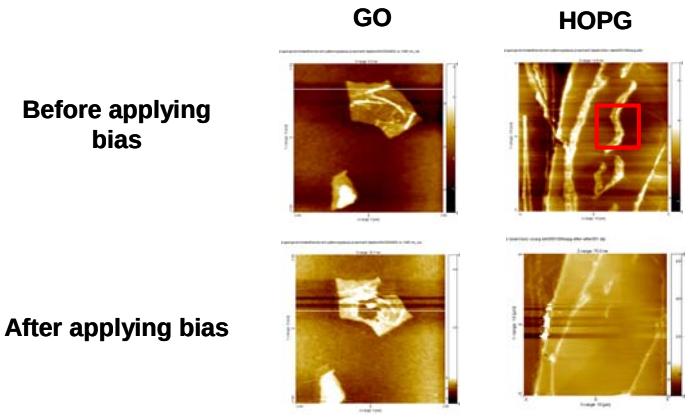

Fig. II-12 Direct comparison between GO and HOPG (330 ^{o}C)

3.2. Friction force of GO and HOPG

Figure II-13 shows the comparison between general cantilever and TCNL cantilever which was seemed to be one of possible problems to measure the friction force. When the general cantilever was used, the friction forces of Si and GO were 550 mV and 250 mV,

respectively. In other words, the difference in friction force was found between Si and GO. However, there is no difference between Si and GO when TCNL cantilever was used. It is thought that general tip is bandable so that it is adequate to measure the friction force. In the case of TCNL cantilever, it is conductive but stiff so that it is not good to measure the friction force. So, general cantilever is seemed to be more adequate to detect the difference of friction force before and after making a pattern with TCNL tip. But, it is thought that measuring the friction force of organic materials with TCNL cantilever is another story.

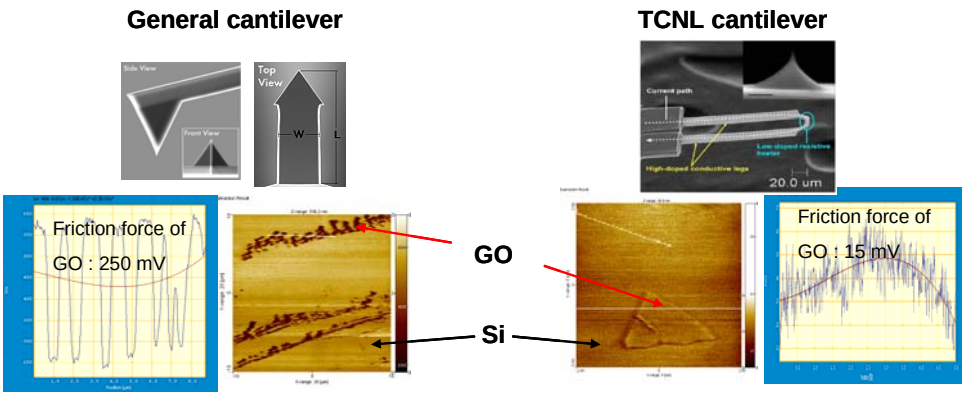

Fig. II-13 General cantilever vs TCNL cantilever

Figure II-14 shows the friction force of GO and HOPG measured by general cantilever. The sum value, starting deflection value, and setting deflection value were 0.67, - 0.2, and 0.1, respectively. Conversion factor was 13.2 nm/V and spring constant of cantilever was 4.5 nN/nm (2.5 ~ 8.5). The friction force of GO is measured to 250 mV, but that of HOPG is measured to 17 mV. In other words, the friction force of HOPG is lower than that of GO, as we expected. This result suggested that it is possible to distinguish the change from GO to graphene using friction force. So, the experiments to measure the friction force difference before and after TCNL treatment on GO with general cantilever are still on going now.

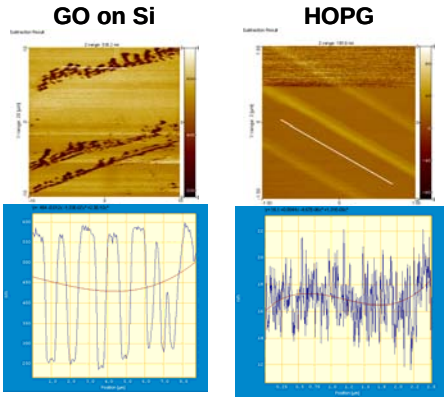

Fig. II-14 Friction force of GO and HOPG measured by general cantilever

4. Poly acrylonitrile

4.1. The purpose of using poly acrylonitrile (PAN)

Figure II-15 shows the method how to change PAN to carbon fiber. It is reported that three steps are needed.[4] First step is stabilization process. In this step, all treatment is conducted at 180 ^{o}C ~ 400 ^{o}C in air. Through this process, structure of PAN changed to that like graphite. Second is carbonization step. This process is conducted at 800 ^{o}C ~ 3000 ^{o}C in nitrogen ambient. Through this process, structure is more changed to that like graphite. The final step is graphitization process at 3000 ^{o}C in argon. This process was a carbonization process at high heating temperature. This method is usually used to make a carbon fiber. So, it is expected that this method can be adopted in our experiment. The goal of this experiment is to change PAN to graphene using TCNL technique.

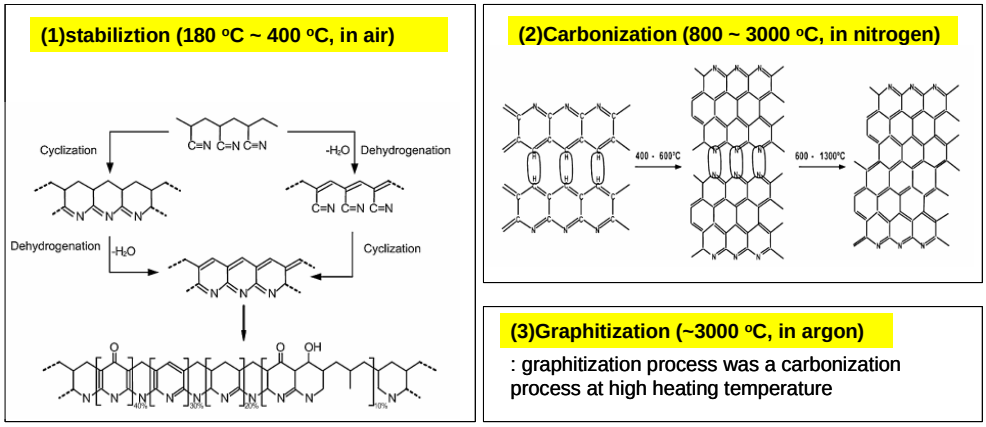

Fig. II-15 The reported method to change PAN fiber to carbon fiber

It is reported that IR spectra are changed after stabilization step. PAN has peaks at 2940 cm^{-1} (-CH stretch), 2240 cm^{-1} (C≡N stretch), 1452 cm^{-1} (-CH_2 bend). After heating at 180 ^{o}C, the intensity of peaks at 2940 cm^{-1} and 2240 cm^{-1} decreased and new peaks appeared at 800 cm^{-1} and 1600 cm^{-1} due to the change of structure. So, it is promising that we can check the change of IR spectra after TCNL treatment on PAN.

4.2. TCNL treatment on PAN

The change of topography and friction images after TCNL treatment on PAN is shown in Fig. II-16. The method reported in reference paper was used in this experiment to make PAN solution.[5] The PAN solution was prepared by dissolving PAN powder in propylene carbonate (boiling temperature: 240 °C) with a concentration of 0.2 and 2 wt % and heated to be transparent at 150 °C. The PAN solution cooled down to room temperature was spin coated on Si substrate at a speed of 1000, 2000, 3000, and 4000 rpm. The PAN-coated substrate was then kept in air at room temperature for 2–20 min. In this experiment, PAN spincoated on Si substrate at the speed of 1000 rpm with 2 wt% was used. After the temperature was increased over than 363 ^{o}C, indentation was found. This indicates that something happened after heat treatment. We are still working on this and further experiments (such as glazing IR or micro IR) are needed.

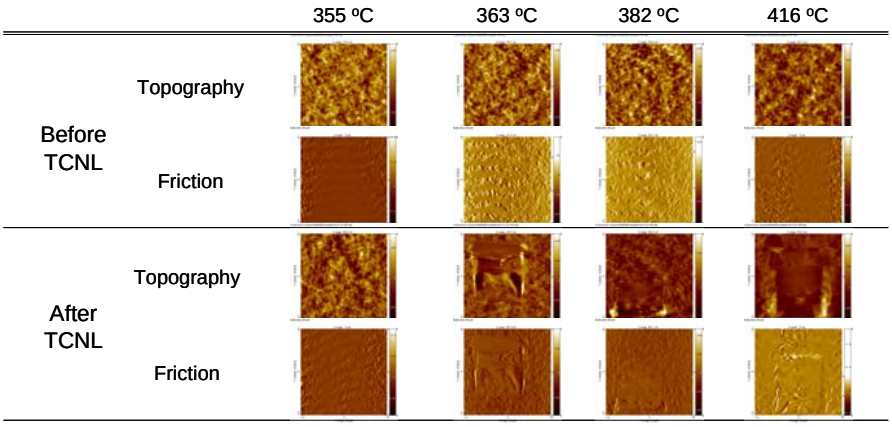

Fig. II-16 The change of topography and friction images after TCNL treatment on PAN

5. Conclusion

It is found that cantilever force affect on the formation of holes in GO as well as temperature. Starting deflection value, setting deflection value, and scanning time were changed to investigate the effect of cantilever force on the formation of hole in GO. The friction force of HOPG is turned out to be lower than that of GO, suggesting that it is possible to detect the change from GO to G using friction force. The change of topography and friction force was found after TCNL treatment on PAN. However, further detailed experiments are needed.

6. Future plan

The purpose of this experiment is to write graphene wires on a GO substrate using TCNL. Until now, TCNL technique to modulate the bad gap of GO is not established well. So, we would like to optimize the TCNL conditions in which the friction force is not recovered. In particular, we will investigate the kinetics of this reaction (by varying the temperature and the writing speed) and the local structure of GO and subsequent graphene structures by means of tip-enhanced Raman spectroscopy and other AFM based electrical measurements. These techniques are particularly indicated for *in-situ* spectroscopic and electric measurements on the fabricated nanostructures. After that, we will design the mask to fabricate the electrode on Si substrate, followed by measuring the current-density voltage curve after TCNL on GO to investigate the change of bandgap.

In the case of PAN, we will use micro IR which is located in Joe Perry's group after TCNL measurement to find the change of structure. First, we will prepare various kinds of sample according to PAN wt% and spin coat speed. In order to find the location easily, patterned sample will be used. After that, 50×50 μm^2 pattern will be made by TCNL according to tip temperature. Finally, we will use micro IR to detect the change of structure.

7. References

[1] S. Y. Zhou, G.-H. Gweon, A. V. Fedorov, P. N. First, W. A. De Heer, D.-H. Lee, F. Guinea, A. H. Castroneto, and A. Lanzara, Nat. Mater. **6**, 770 (2007).

[2] S. Stankovich, D. A. Dikin, R. D. Piner, K. A. Kohlhaas, A. Kleinhammes, Y. Jia, Y. Wu, S. T. Nguyen, and R. S. Ruoff, Carbon **45**, 1558 (2007).

[3] R. Szoszkiewicz, T. Okada, S. C. Jones, T.-D. Li, W. P. King, S. R. Marder, and E. Riedo, Nano Lett. **7**, 1064 (2007).
[4] M.S.A. Rahaman, A.F. Ismail, and A. Mustafa, Polymer degradation and stability **92**, 1421 (2007).
[5] H.-L. Hsu, W.-C. Yang, Y.-L. Lee, and T.-R. Yew, Appl. Phys. Lett. **91**, 023501 (2007).